ELSEVIER

Nuclear Physics A 690 (2001) 755–768

NUCLEAR PHYSICS A

www.elsevier.nl/locate/npe

The ^{14}N(p,γ)^{15}O low-energy S-factor

C. Angulo [a], P. Descouvemont [b,1]

[a] *Centre de Recherches du Cyclotron, Chemin du cyclotron 2, Université catholique de Louvain, B-1348 Louvain-la-Neuve, Belgium*

[b] *Physique Nucléaire Théorique et Physique Mathématique CP229, Université Libre de Bruxelles, B-1050 Brussels, Belgium*

Received 13 November 2000; revised 4 December 2000; accepted 14 December 2000

Abstract

The ^{14}N(p,γ)^{15}O low-energy S-factor is analyzed using the R-matrix model. We find that the g.s. contribution is less than previously reported. The S-factor is mainly given by the 6.79 MeV state contribution which is determined by its asymptotic normalization constant (ANC). Consequently, the S-factor at zero energy is lower by a factor of 1.7 compared to the values given in recent compilations. This result may affect the nucleosynthesis and time scale evolution in massive stars. New measurements of the ^{14}N(p,γ)^{15}O cross section over a wide energy range, and especially at low energies, are highly desirable. Significant improvement could be also obtained from the ANC measurement of the 6.79 MeV state.

PACS: 24.10.-i; 25.40.Lw; 25.40.Qa; 26.20.+f
Keywords: ^{14}N(p,γ)^{15}O cross section; R-matrix; Reaction rate

1. Introduction

The ^{14}N(p,γ)^{15}O reaction is the slowest one in the hydrogen burning CN-cycles. In a massive main-sequence star, this reaction plays the role of setting the energy generation and, consequently, the time scale for its evolution. In particular, a change in its rate would have a significant influence on the structure and nucleosynthesis of the star during the hydrogen and helium phases [1]. The ^{14}N(p,γ)^{15}O cross section has been measured by several groups during the last 50 years [2–6], but only the measurements of Schröder et al. [6] extend over a wide energy range, for laboratory energies $E_{\rm p} = 0.2$ to 3.6 MeV. According to these authors, the main contribution to the S-factor at zero energy comes from transitions to the $1/2^-$ ground-state in ^{15}O and to the $3/2^+$ subthreshold state at $E_x = 6.79$ MeV ($E_{\rm cm} = -0.504$ MeV). From extrapolations to astrophysical energies,

E-mail address: angulo@cyc.ucl.ac.be (C. Angulo).
[1] Directeur de Recherches FNRS

0375-9474/01/$ – see front matter
PII: S0375-9474(00)00696-5

Schröder et al. find a significant contribution from the subthreshold state, and only a negligible contribution from capture to the $3/2^-$ state at $E_x = 6.18$ MeV. This implies that the reaction rate at temperatures $T \leqslant 3 \times 10^8$ K is dominated by the tail of the $3/2^+$ subthreshold state, but sensitively depends on its width, which is presently not well established. Recent experiments [7] aimed at determining the mean lifetime of the 6.79 MeV state, lead to a γ-width smaller than previously accepted and, consequently, to lower values of the extrapolated S-factor at astrophysical energies. At temperatures $T \geqslant 3\times10^8$ K, the $1/2^+$ resonance at $E_\mathrm{r} = 0.259$ MeV dominates the reaction rate. Interference effects between several $3/2^+$ higher energy lying resonances must also be considered [8]. As stated in [9], the uncertainty in the reaction rate is, therefore, most probably greater than the accepted values.

In this paper, we analyze the low-energy radiative capture (RC) data of Schröder et al. using the R-matrix theory [10]. In this method, the physics of the problem is determined by the properties (energy, proton and γ widths) of some poles. Although the poles are related to physical properties of resonances or bound states, their properties are not directly linked to the experimental data. The main drawback of the R-matrix method is that the link between the "formal", or "calculated", properties and the "observed" properties, which correspond to the experimental data, is not straightforward. In a recent paper [11], we have developed a new method to derive "formal" inputs from experimental data. We have used this new approach in the present analysis of the ^{14}N(p,γ)^{15}O cross section.

In Section 2, the R-matrix formalism is briefly explained. The results of our analysis and a comparison with previous results are presented in Section 3. Some astrophysical implications and conclusions are drawn in Section 4.

2. Summary of the R-matrix formalism

2.1. Elastic scattering

In this section, we briefly present the main inputs to the R-matrix theory. Additional information can be found, for instance, in Refs. [10–12]. We assume here that, for a given partial wave $J\pi$, a single channel spin I ($1/2$ or $3/2$, resulting from the coupling of ^{14}N and proton spins) and a single ℓ value contribute. This approximation is justified at low energies where only the lowest angular momentum is expected to be significant; above the Coulomb barrier, some mixing may occur, but this effect is beyond the scope of the present work where we focus on astrophysical energies. In this approximation, the R-matrix at energy E is defined by

$$R(E) = \sum_{\lambda=1}^{N} \frac{\tilde{\gamma}_\lambda^2}{E_\lambda - E}, \tag{1}$$

where $\tilde{\gamma}_\lambda^2$ and E_λ are the calculated proton reduced width and the energy of the pole λ, and N is the number of poles. For the sake of clarity, we do not explicitly write angular momenta as labels. From the R-matrix, one deduces the collision matrix

$$U(E) = \frac{I(ka)}{O(ka)} \frac{1 - L(E)^* R(E)}{1 - L(E) R(E)} = \exp\bigl(2i\delta(E)\bigr), \tag{2}$$

where I and O are the ingoing and outgoing Coulomb functions, k is the wave number and a is the R-matrix radius. Constant $L(E)$ does not depend on r and is defined as

$$L(E) = ka \frac{O'(ka)}{O(ka)}, \tag{3}$$

and $\delta(E)$ is the phase shift.

The R-matrix parameters E_λ and $\tilde{\gamma}_\lambda^2$ are related to experimental energies and proton widths, but the relationship is not simple when $N > 1$. In Ref. [11], we have developed a new iterative method which enables to switch between R-matrix parameters ("calculated" or "formal" parameters) to experimental data ("observed" parameters). This technique assumes that the levels are well separated, which is valid here. It is particularly suited when the parameter set is constrained by well-known data. In the present case, ^{15}O energies are taken from the literature [13] and are not considered as free parameters.

2.2. Capture cross sections

Capture cross sections involve matrix elements of the electromagnetic operator $\mathcal{M}_L^\sigma$, ($\sigma = E$, electric, or M, magnetic) of order L. In the internal region, where the relative distance r between the colliding nuclei is less than a, the radial part of the wave function is

$$\psi_{\rm int}(r) = \sum_\lambda f_\lambda \chi_\lambda(r), \quad r \leqslant a, \tag{4}$$

where $\chi_\lambda(r)$ are the basis functions defining the pole properties [10,11], and f_λ are variational parameters. In the external region, the wave function is an exact solution of the Schrödinger equation with the Coulomb potential, and is defined as

$$\begin{aligned} \psi_{\rm ext}(r) &= [F(kr)\cos\delta + G(kr)\sin\delta], \quad r \geqslant a, \qquad E > 0, \\ &= C W_{-\eta,\ell+\frac{1}{2}}(2kr), \quad r \geqslant a, \qquad E < 0, \end{aligned} \tag{5}$$

where F and G are the Coulomb functions, W is the Whittaker function and C is the asymptotic normalization constant (ANC). For bound states, the wave function is normalized to unity over the whole space.

The capture cross section to a final (bound) state with spin J_f and parity π_f is given by

$$\sigma(E, J_i\pi_i \to J_f\pi_f) = \frac{\pi}{k^2} \frac{2J_i + 1}{(2I_1 + 1)(2I_2 + 1)} |M_{\rm int} + M_{\rm ext}|^2, \tag{6}$$

where I_1 and I_2 are the spin of the colliding nuclei [14]. The internal matrix element $M_{\rm int}$ is

$$M_{\rm int} = \frac{\sum_\lambda \varepsilon_\lambda [\widetilde{\Gamma}_\lambda(E) \widetilde{\Gamma}_\lambda^\gamma(E)]^{1/2} / (E_\lambda - E)}{|1 - LR(E)|}, \tag{7}$$

where $\widetilde{\Gamma}_\lambda(E)$ is the total width of the pole λ, $\widetilde{\Gamma}_\lambda^\gamma(E)$ is the formal gamma width, and ε_λ is a phase factor ($+1$ or -1). The external contribution is given by

$$M_{\rm ext} = C\left[Z_1\left(\frac{A_2}{A}\right)^L + Z_2\left(-\frac{A_1}{A}\right)^L\right]K_{if} \times \int_a^\infty [F_{\ell_i}(kr)\cos\delta + G_{\ell_i}(kr)\sin\delta]W_{-\eta,\ell_f+\frac{1}{2}}(2k_f r)r^L dr, \tag{8}$$

where the geometrical factor K_{if} is

$$K_{if} = e\left[\frac{8(L+1)(2L+1)}{L\hbar v}k_\gamma^{2L+1}(2\ell_i+1)(2\ell_f+1)(2J_f+1)\right]^{1/2} \times \frac{1}{(2L+1)!!}\begin{pmatrix}\ell_f & L & \ell_i\\ 0 & 0 & 0\end{pmatrix}\begin{Bmatrix}J_i & \ell_i & I\\ \ell_f & J_f & L\end{Bmatrix}. \tag{9}$$

In these expressions, we have introduced the initial and final angular momenta, with labels i and f, respectively, the relative velocity v, and the photon wave number k_γ.

For deeply bound states, such as the ^{15}O ground state, the external contribution is expected to play a minor role since the Whittaker function decreases rapidly for large r values. However, this term is dominant for weakly bound states. A well-known example is the ^{7}Be(p,γ)^{8}B reaction where the ^{8}B ground state is bound by only 137 keV, and where the capture matrix elements are essentially given by the long-range part of the wave functions. In this case, the unknown quantities are the asymptotic normalization constant C and, to a lesser extent, the phase shift [15]. Notice that the internal and external terms are not independent of each other since the phase shift, determined from the R-matrix parameters, appears in the external matrix element.

2.3. Relationship between ANC and R-matrix parameters

When a capture reaction proceeds to a weakly bound state, the cross section is essentially determined by the ANC [16,17]. On the other hand, such a subthreshold state may also be important in capture towards another state. This situation occurs in the ^{12}C(α,γ)^{16}O reaction, for example, where the 1^- and 2^+ subthreshold states are well known to have an affect on the low-energy S-factor. The influence of a subthreshold state appears through its reduced width and its gamma width.

In the single-pole approximation, the "formal" reduced width $\widetilde{\gamma}_\lambda^2$ is related to the basis function $\chi_\lambda(r)$ through [10]

$$\widetilde{\gamma}_\lambda^2 = \frac{\hbar^2}{2\mu a}\chi_\lambda^2(a), \tag{10}$$

where $\chi_\lambda(r)$ is normalized to unity in the internal region. Comparison of (5) and (10) yields

$$\big(CW(a)\big)^2 = \frac{2\mu a}{\hbar^2}\frac{\widetilde{\gamma}_\lambda^2}{N}, \tag{11}$$

where N is the integral of $\chi_\lambda^2(r)$ over the whole space, including the external region (indexes of the Whittaker function have been dropped). We have

$$N = 1 + \chi_\lambda(a)^2 \int_a^\infty \left(\frac{W(r)}{W(a)}\right)^2 dr = 1 + \widetilde{\gamma}_\lambda^2 \frac{dS}{dE}, \tag{12}$$

where S is the shift factor [10]. In the single-pole approximation, the "observed" reduced width γ_λ^2 is related to the "formal" reduced width $\widetilde{\gamma}_\lambda^2$ by

$$\gamma_\lambda^2 = \frac{\widetilde{\gamma}_\lambda^2}{1 + \widetilde{\gamma}_\lambda^2 (dS/dE)}. \tag{13}$$

Consequently, we find the relationship between C and the "observed" reduced width γ_λ^2

$$C^2 = \frac{2\mu a}{\hbar^2 W^2(a)} \gamma_\lambda^2, \tag{14}$$

which can be used either to derive one parameter from the other one or to check the consistency of both parameters. In the present study, this equation will be used to test parameters of the 6.79 MeV level, located 504 keV below the $^{14}\mathrm{N} + \mathrm{p}$ threshold.

3. Results and discussion

We have analyzed capture data [6] to the $1/2^-$ ground-state, the 6.18 $(3/2^-)$ and 6.79 $(3/2^+)$ MeV states up to 2.5 MeV, using the R-matrix model explained in Section 2, with $a = 6.5$ fm. The sensitivity of the results to this choice of the radius is rather low, and much lower than the experimental uncertainties. According to Schröder et al., contributions to the total cross section of transitions to the states at 5.18 $(1/2^+)$, 5.24 $(5/2^+)$, 6.86 $(5/2^+)$, and 7.28 $(7/2^+)$ MeV account for less than 3% of the total zero-energy cross section and have not been considered here. In each case, the ε_λ values are considered as free parameters ($+1$ or -1).

3.1. Ground-state transitions

Capture data for transitions to the ^{15}O ground-state involve the E1 contributions from s-waves, i.e., from the $1/2^+$ resonance at $E_\mathrm{r} = 0.259$ MeV, from the two $3/2^+$ resonances at $E_\mathrm{r} = 0.985$ and 2.187 MeV, and from the $3/2^+$ subthreshold state at $E = -0.504$ MeV. In order to account for higher energy resonances, we have included a background pole ($\ell_i = 0$) at $E = 5.0$ MeV for both the $1/2^+$ and $3/2^+$ components. The external contribution to the matrix elements is taken into account through the parameter C (Eq. (14)). All resonance energies are taken from the literature [13], all proton and γ-widths are left as free parameters. The parameters of the fit are given in Table 1. The best fit, which corresponds to $\varepsilon_\lambda = +1$ for all resonances, is shown in Fig. 1 as a full curve (all other sets of ε_λ values do not give satisfactory fits). The sensitivity to the external capture is very low and the fit is consistent with $C = 0$.

Table 1
Observed R-matrix parameters for capture transitions to the ground-state and to the states at $E_x = 6.18$ and 6.79 MeV

		E_r (MeV)	Γ_p (keV)	Γ_γ (eV)	ε_λ
RC → g.s.	$J_i^{\pi_i} = 1/2^+$	0.2594	1.0 ± 0.1	$(1.60 \pm 0.20) \times 10^{-3}$	+1
	$J_i^{\pi_i} = 3/2^+$	−0.504	140 ± 30[a]	1.75 ± 0.60	+1
		0.985	3.0 ± 1.0	0.10 ± 0.03	+1
		2.187	270 ± 10	9.0 ± 0.2	+1
		5.0	4800 ± 500	82.0 ± 8.0	+1
RC → 6.18 MeV	$J_i^{\pi_i} = 1/2^+$	0.2594	1.0 ± 0.1	$(2.0 \pm 0.4) \times 10^{-2}$	+1
		1.446	42 ± 10	0.11 ± 0.02	−1
		5.0	3120 ± 1040	30 ± 10	+1
	$J_i^{\pi_i} = 3/2^+$	−0.504	140 ± 30[a]	$(5.0 \pm 3.0) \times 10^{-3}$	+1
		0.985	3.0 ± 1.0	$(4.0 \pm 2.0) \times 10^{-3}$	−1
		2.187	270 ± 10	0.33 ± 0.07	−1
RC → 6.79 MeV	$J_i^{\pi_i} = 1/2^+$	0.2594	1.0 ± 0.1	$(1.0 \pm 0.1) \times 10^{-2}$	+1
$C = 5.6$ fm$^{-1/2}$	$J_i^{\pi_i} = 1/2^-, 3/2^-, 5/2^-$[b]	–	–	–	

[a] Reduced width, γ^2.

[b] External capture only.

This fit is obtained without contribution of the background pole in the $1/2^+$ component. We obtain a reduced width of the subthreshold state $\gamma_1^2 = 0.14$ MeV which is 9% of the Wigner limit. The fitted γ-width, $\Gamma_\gamma = 1.75$ eV, is 3.6 times smaller than the value given in [6], but much larger than the lower limit given in compilations, $\Gamma_\gamma > 0.024$ eV [13]. For the resonance at $E_r = 0.985$ MeV, we obtain a proton width $\Gamma_p = 3.0$ keV, in good agreement with previous results [5,6,18]; however, the γ-width $\Gamma_\gamma = 0.10$ eV is a factor of 2.4 lower than the value given in [13]. Notice that the fit is very sensitive to the energy of this resonance. The best fit is obtained for an energy 2 keV lower than the value given in literature. The proton width of the $E_r = 2.187$ MeV resonance is about 40% larger than the value given in literature [13]. Notice that the $\ell_i = 0$ assumption has been used for this resonance, but a $\ell_i = 2$ contribution could be non-negligible [6].

The error in $S(0)$ has been estimated by varying the parameters of the subthreshold state and of the background pole. In fact, the χ^2 values essentially depend on the products $\gamma_1^2 \times \Gamma_\gamma^1$ and $\Gamma_p^4 \times \Gamma_\gamma^4$. In both cases, variations of the product by about 40% change the χ^2 by a few percents, but affect $S(0)$ significantly. In other words, the sensitivity of $S(0)$ is much stronger than the sensitivity of the global χ^2. As an illustrative example, Fig. 2 shows the sensitivity of the S-factor with respect to the proton and γ widths of the subthreshold state for energies $E \leqslant 1$ MeV (above 1 MeV, the curves are not distinguishable). Although the S-factor at zero energy is changed by more than a factor 2, the quality of the fit remains almost unchanged. Similar conclusions are obtained by considering variations of the background properties. The R-matrix fit leads to a S-factor at zero energy $S(0) =$

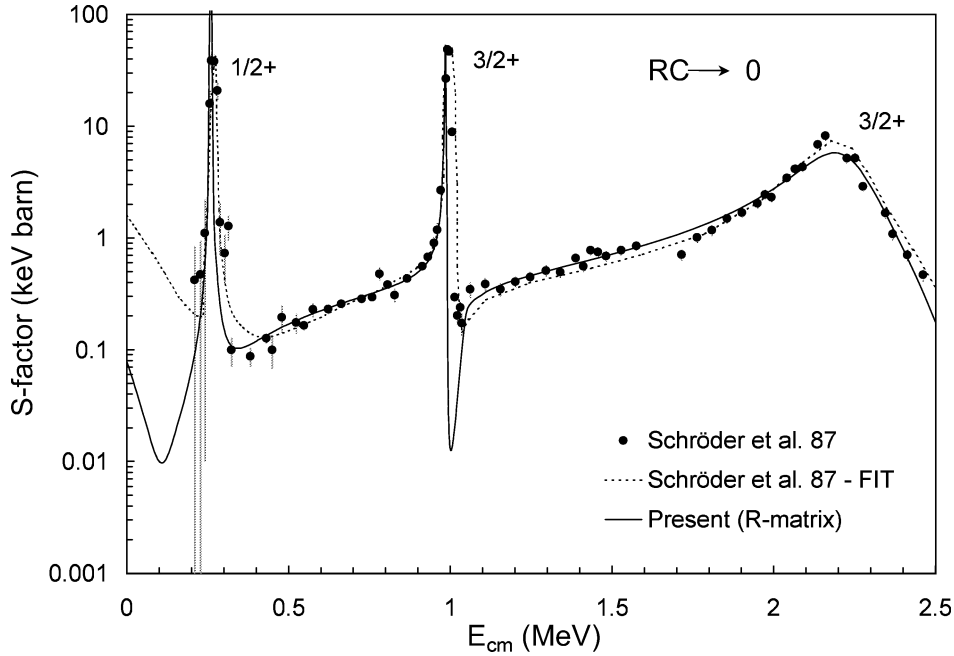

Fig. 1. The S-factor data of the ^{14}N(p,γ)^{15}O reaction for the capture process into the ground-state of ^{15}O from Ref. [6] is shown together with the R-matrix fits. The full curve represents the best fit (see text). The dotted curve is the fit of Schröder et al. [6].

$0.08^{+0.13}_{-0.06}$ keV b, where the error bar accounts for uncertainties on the subthreshold-state and background parameters. This $S(0)$ is about 20 times smaller than the value obtained by Schröder et al. [6].

On the other hand, in an attempt to understand the results of Schröder et al., we have used their resonance parameters to perform a R-matrix calculation. We have included a background pole fixed at 5.0 MeV. The free parameters of the fit are the proton reduced width of the subthreshold state γ_1^2, not given in [6], and the proton, Γ_p^4, and γ, Γ_γ^4, widths of the background pole. Our best fit does not agree with the data at the energies where this analysis is performed ($E \leqslant 2.5$ MeV). We did not find any parameter set which reproduces the fit of Schröder et al., shown as a dotted curve in Fig. 1.

3.2. Transitions to the 6.18 MeV state

For transitions to the 6.18 MeV state ($3/2^-$), we include E1 contributions from the $1/2^+$ resonances at $E_\mathrm{r} = 0.259$ and 1.446 MeV, E1 contributions from the $3/2^+$ resonances at $E_\mathrm{r} = 0.983$ and 2.187 MeV, and from the $3/2^+$ subthreshold state at $E = -0.504$ MeV, as well as background poles for each J^π component.

Resonance energies are taken from the literature [13], and proton and γ-widths are left as free parameters. The parameters of the best fit are given in Table 1; again the data are not accurate enough to derive the ANC. The best fit is obtained for a zero contribution of

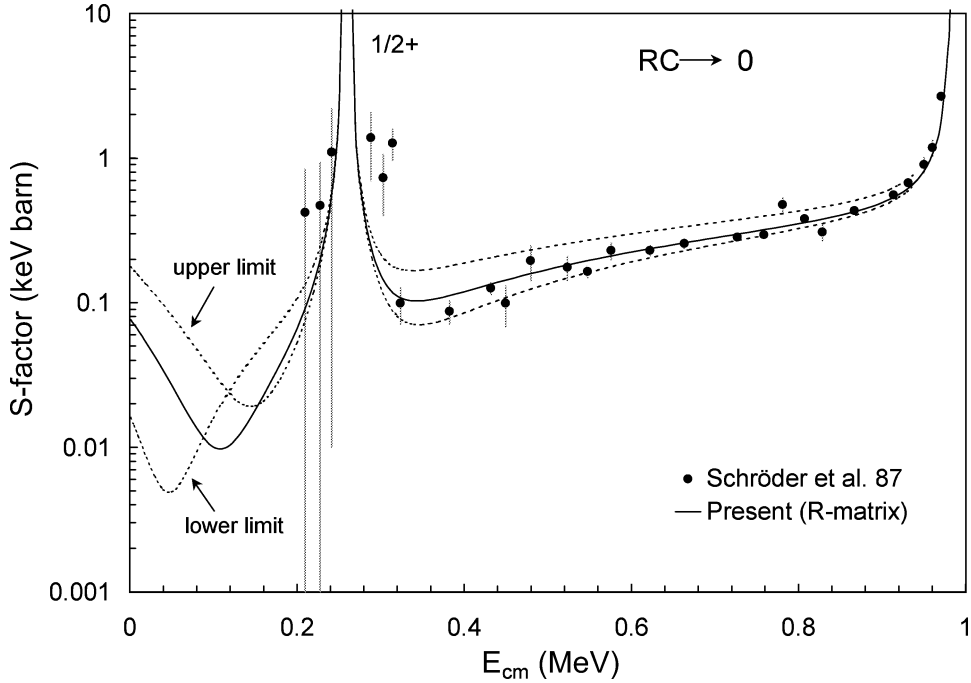

Fig. 2. Low-energy S-factor of ^{14}N(p,γ)^{15}O for the capture process into the ground-state of ^{15}O [6]. The lower and upper limits have been calculated by changing the parameters of the subthreshold state (see text).

the background pole in the $3/2^+$ component. The resulting parameters for all resonances are in good agreement with the values of nuclear data compilations [13].

The best fit is shown in Fig. 3 (full curve) together with the data of Schröder et al. [6]. Since the energy difference is small, the γ-width of the subthreshold state, $\Gamma_\gamma = 5.0 \times 10^{-3}$ eV is very low and, thus, the contribution of this state is not important for this transition. We have estimated that a change of about 40% in the product $\Gamma_p^1 \times \Gamma_\gamma^1$ does not change the fit significantly. The resulting S-factor at zero energy is $S(0) = 0.06^{+0.01}_{-0.02}$ keV b, about 2.3 times lower than the value given in [6] due to the lower contribution of the subthreshold state found here. This value is also more than 16 times lower than the value given by Hebbard and Bailey [5]. Consequently, transitions to the 6.18 MeV state contribute less than 3.5% to the total S-factor at $E = 0$.

3.3. Transitions to the 6.79 MeV state

The $1/2^+$ resonance at 0.259 MeV decays to the 6.79 MeV state by E2 radiation. The non-resonant part of the data can be explained by an E1 contribution from the $J_i^{\pi_i} = 1/2^-, 3/2^-$ and $5/2^-$ partial waves ($\ell_i = 1$); since the 6.79 MeV state is weakly bound and since no resonance decays by E1 multipolarity, only the external part of the matrix elements is included. The parameters of the best fit are given in Table 1. Fig. 4 shows the best fit compared to the data of Schröder et al. [6]. Notice that the inclusion of

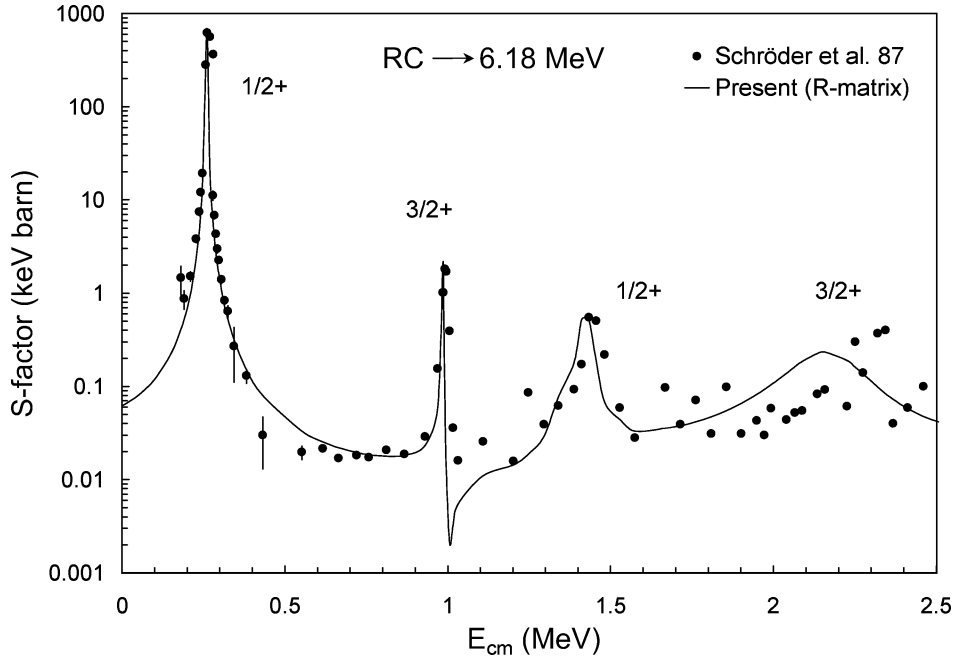

Fig. 3. The S-factor data of the ^{14}N(p,γ)^{15}O reaction for the capture process into the 6.18 MeV state of ^{15}O from Ref. [6] are shown together with the best fit (see text).

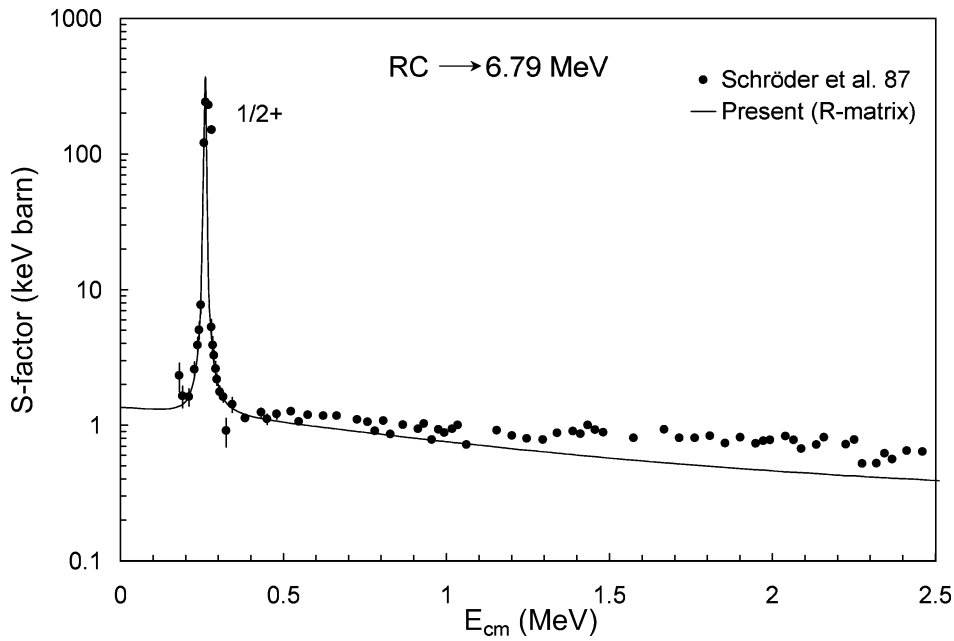

Fig. 4. The S-factor data of the ^{14}N(p,γ)^{15}O reaction for the capture process into the 6.79 MeV state of ^{15}O from Ref. [6] are shown together with the best fit (see text).

a background pole would give a better fit for energies above 1 MeV, but will not change the conclusions for the lower energies. We obtain a value of the S-factor at zero energy of $S(0) = 1.63 \pm 0.17$ keV b, which is the main contribution to the total S-factor of the ^{14}N(p,γ)^{15}O capture process. This value is in fair agreement with the result of Schröder et al. [6] ($S(0) = 1.41$ keV b). The 10% uncertainty is mainly due to experimental errors.

The ANC value deduced from the capture data for the 6.79 MeV level ($J_f^{\pi_f} = 3/2^+$) is $C = 5.6$ fm$^{-1/2}$ (see Table 1). Using the reduced width obtained from capture from the $3/2^+$ partial waves ($\gamma^2 = 0.14$ MeV — see Table 1) gives

$$C = 4.2 \text{ fm}^{-1/2} \tag{15}$$

from Eq. (14). Although obtained by quite different procedures, both values are consistent with each other. The 30% difference can be explained by experimental uncertainties and from theoretical approximations, such as the single-pole approximation to derive Eq. (14). Since the 6.79 MeV level provides the main contribution to the ^{14}N(p,γ)^{15}O low-energy cross section, the quantity C appears to be the most important input. Contrary to the conclusions of [6], these results, together with the results for the transitions to the g.s and the 6.18 MeV state, show that the total capture process is largely dominated by transitions to the state at 6.79 MeV, and that transitions to the ground-state account for only 5% of the total S-factor at zero energy.

3.4. The total S-factor at low energies

The $S(E)$ values extrapolated to zero energy for transitions to the ^{15}O bound states (g.s., 6.18, and 6.79 MeV, respectively) are presented and compared with the results of Hebbard and Bailey [5] and Schröder et al. [6] in Table 2. The $S(0)$ value for capture into the 6.79 MeV state is the main contribution to the total S-factor, and it is in fair agreement with previous results [5,6,9]. On the other hand, the contribution of transitions to the 6.18 MeV state is found to be minor compared to reported values. The main difference concerns the $S(0)$ factor for capture to the ^{15}O ground-state. Although rather uncertain, the present value $S(0) = 0.08$ keV b is more than a factor of 19 lower than the value of Schröder et al. [6], but the upper limit is similar to the value reported by Hebbard and Bailey [5]. This discrepancy is due to the fact that, for transitions to the ground-state, we

Table 2
Summary of $S(0)$ values (in units of keV b)

Transition (MeV)	Hebbard and Bailey Ref. [5]	Schröder et al. Ref. [6]	Present R-matrix calc.
RC $\rightarrow$ 0	0.27	1.55 ± 0.34	$0.08^{+0.13}_{-0.06}$
RC $\rightarrow$ 6.18	1.00	0.14 ± 0.05	$0.06^{+0.01}_{-0.02}$
RC $\rightarrow$ 6.79	1.40	1.41 ± 0.02	1.63 ± 0.17
Total	2.67	3.10 ± 0.34	1.77 ± 0.20

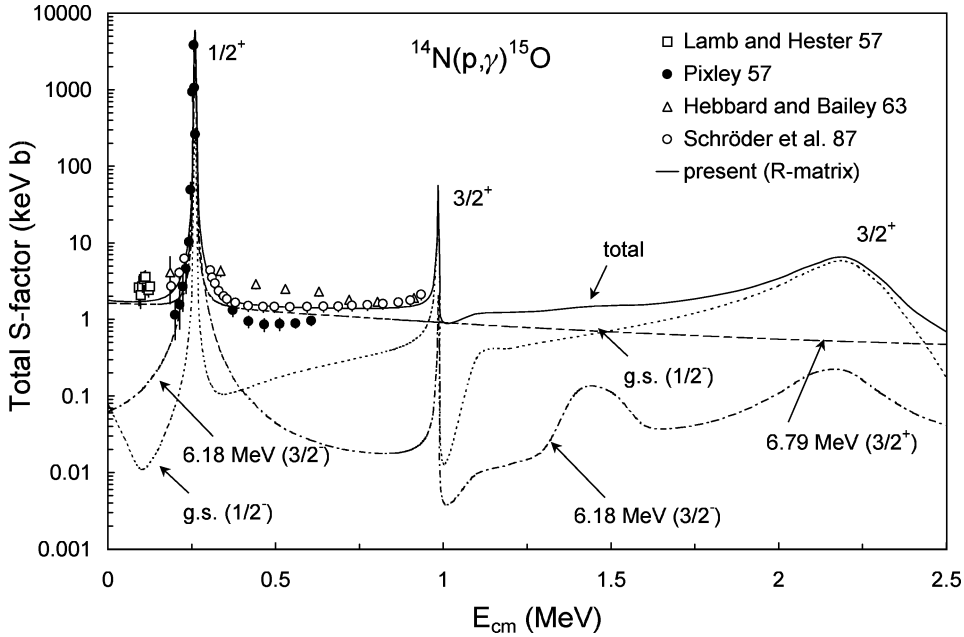

Fig. 5. Total S-factor for the reaction ^{14}N(p,γ)^{15}O. The curves represent the results of the R-matrix analysis for energies $E \leqslant 2.5$ MeV. The data are from Refs. [2–6]

find that the 6.79 MeV subthreshold state is not as important as predicted by [6]. Although this subthreshold state has an observable γ-width, $\Gamma_\gamma = 1.75$ eV, the proton reduced width γ_1^2 is probably much lower than the value obtained in [6], but no explanation is given there for the procedure of obtaining γ_1^2 from spectroscopy factors. From this analysis, the recommended S-factor at zero energy is $S(0) = 1.77 \pm 0.20$ keV b, which is a factor of 1.7 lower than the values used in recent compilations [8,9].

The total S-factor of the ^{14}N(p,γ)^{15}O capture reaction resulting from the present R-matrix analysis for $E \leqslant 2.5$ MeV is shown in Fig. 5, together with the data taken from literature [2–6]. The contribution of transitions to the g.s, the 6.18 MeV, and the 6.79 MeV states are also shown. As discussed above, the transition to the 6.79 MeV state dominates the S-factor. At low energies, the contribution of the g.s. and the 6.18 MeV state are minor, and the global uncertainties come mainly from the uncertainties due to 6.79 MeV transitions, that are of the order of the experimental errors. Notice that even if the uncertainties of the subthreshold state parameters for the g.s. and the 6.18 MeV transitions are large, they do not play a significant role. However, at energies above 1 MeV, transitions to the g.s. are important, especially near the $3/2^+$ resonance at 2.187 MeV.

3.5. The $^{14}N(p,\gamma)^{15}O$ reaction rate

The Maxwellian averaged reaction rates (in cm^3 mole^{-1} s^{-1}) are computed (Table 3) from [8]:

Table 3
^{14}N(p,γ)^{15}O reaction rates in cm^3 mole^{-1} s^{-1} for temperatures of $0.005 \leqslant T_9 \leqslant 2$

T_9	$N_A\langle\sigma v\rangle$	T_9	$N_A\langle\sigma v\rangle$	T_9	$N_A\langle\sigma v\rangle$	T_9	$N_A\langle\sigma v\rangle$
0.005	1.9×10^{-30}	0.018	2.2×10^{-17}	0.12	5.2×10^{-06}	0.45	$1.8 \times 10^{+01}$
0.006	3.2×10^{-28}	0.02	1.5×10^{-16}	0.13	1.8×10^{-05}	0.5	$3.0 \times 10^{+01}$
0.007	1.9×10^{-26}	0.025	7.4×10^{-15}	0.14	5.7×10^{-05}	0.6	$6.3 \times 10^{+01}$
0.008	5.7×10^{-25}	0.03	1.4×10^{-13}	0.15	1.8×10^{-04}	0.7	$1.0 \times 10^{+02}$
0.009	9.8×10^{-24}	0.04	1.0×10^{-11}	0.16	5.2×10^{-04}	0.8	$1.5 \times 10^{+02}$
0.01	1.1×10^{-22}	0.05	2.2×10^{-10}	0.18	3.3×10^{-03}	0.9	$1.9 \times 10^{+02}$
0.011	9.8×10^{-22}	0.06	2.2×10^{-09}	0.2	1.4×10^{-02}	1	$2.2 \times 10^{+02}$
0.012	6.5×10^{-21}	0.07	1.4×10^{-08}	0.25	2.1×10^{-01}	1.25	$3.0 \times 10^{+02}$
0.013	3.6×10^{-20}	0.08	6.3×10^{-08}	0.3	$1.2 \times 10^{+00}$	1.5	$3.6 \times 10^{+02}$
0.014	1.6×10^{-19}	0.09	2.3×10^{-07}	0.35	$3.9 \times 10^{+00}$	1.75	$4.1 \times 10^{+02}$
0.015	6.6×10^{-19}	0.1	7.0×10^{-07}	0.4	$9.3 \times 10^{+00}$	2	$4.4 \times 10^{+02}$
0.016	2.4×10^{-18}	0.11	1.8×10^{-06}				

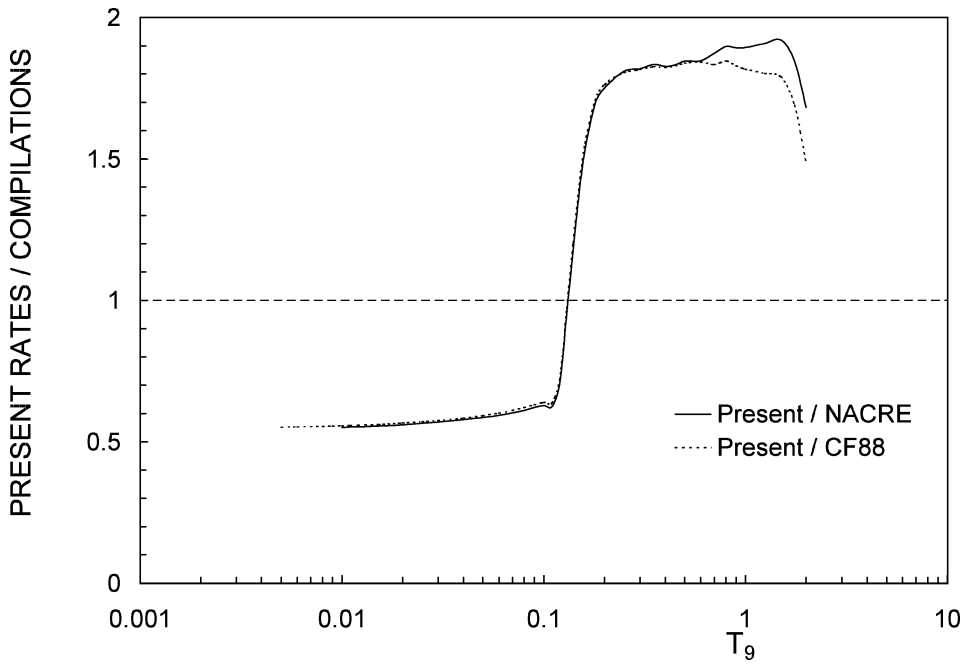

Fig. 6. Present rates compared to the NACRE and the CF88 rates for temperatures of $0.005 \leqslant T_9 \leqslant 2$ (see text).

$$N_A\langle\sigma v\rangle = 3.7313 \times 10^{10}\, \mu^{-1/2}\, T_9^{-3/2} \times \int_0^\infty S(E) \exp(-2\pi\eta) \exp(-11.605E/T_9) dE, \quad (16)$$

where μ is the reduced mass of the system in amu, T_9 is the temperature in units of 10^9 K, E is the c.m. energy in MeV, and η is the Sommerfeld parameter [19].

The calculation is performed numerically using the S-factor values obtained from the R-matrix fits (Figs. 1 to 4) for temperatures between $T_9 = 0.005$ and 2. Fig. 6 shows the ratio of the present rates compared to those from the NACRE [8] and CF88 [20] compilations. For temperatures below $T_9 = 0.15$, the present rates are lower by about a factor of 2 compared to the NACRE and the CF88 rates. These results can be understood since the S-factor values used here differ by that same amount to the ones used in [8,20], which are based on the results of [6]. On the other hand, for temperatures above $T_9 = 0.15$, the present rates are 50% larger than the NACRE and the CF88 rates. These differences are due to the contribution of the tail of the $1/2^+$ 0.2594 MeV resonance, that was treated as an isolated narrow resonance in [8,20]. For temperatures above $T_9 = 2$, the contribution of higher energy resonances must be included to obtain a reliable rate.

4. Conclusions

We have performed a R-matrix analysis of the S-factor of the ^{14}N(p,γ)^{15}O reaction to the bound states of ^{15}O which mainly contribute to the total cross section (g.s., 6.18 and 6.79 MeV states, respectively). As a result of this analysis, we have obtained properties of several important resonances and of the subthreshold state at $E = -0.504$ MeV, as well as S-factor values for energies $E \leqslant 2.5$ MeV. Two main conclusions can be drawn from this analysis. First, the total capture process is largely dominated by transitions to the state at 6.79 MeV. The ANC value deduced from the capture data for the 6.79 MeV level, $C = 5.6$ fm$^{-1/2}$, appears to be the most important input. Second, the contribution of the subthreshold state for transitions to the ground-state is much lower than previously reported [6]. These results are in agreement with recent experimental data [7]. As a consequence, the zero energy S-factor for the g.s. transition, $S(0) = 0.08$ keV b, is lower than previously accepted values [5,6,8,9].

From the present S-factor values, we have calculated the ^{14}N(p,γ)^{15}O reaction rates in the temperature range $0.005 \leqslant T_9 \leqslant 2$ and compared them to the NACRE [8] and the CF88 [20] rates. The present rates differ from the NACRE and CF88 rates by a factor of about 2 at temperatures below $T_9 = 0.15$. The present results may have an important influence on the nucleosynthesis of main sequence stars during the hydrogen and helium burning phases. According to Ref. [1], a reduction of the ^{14}N(p,γ)^{15}O rate at temperatures of the order of $T \leqslant 3 \times 10^8$ K by a factor 2 implies that the CNO cycle, even though operating in equilibrium, operates at a slightly higher temperature. This fact is enough to introduce an effect on the amount of ^{17}O, which is destroyed more efficiently, and to produce a slightly higher enrichment of ^{22}Na. Therefore, there exists a direct link between the destruction of ^{14}N via the capture process and the cycles operating at higher temperatures.

New measurements of the ^{14}N(p,γ)^{15}O cross section at energies $E \leqslant 2$ MeV are desirable. In particular, new measurements of transitions to the $3/2^+$ state (6.79 MeV) should

be performed and extended to lower energies. Indirect measurements of the properties of resonances and of the 6.79 MeV subthreshold state would also give useful complementary information.

Acknowledgements

We are grateful to J.S. Schweitzer for a careful reading of the manuscript. We thank C.R. Brune and A.E. Champagne for interesting discussions. This paper presents research results of the Belgian Program P4/18 on interuniversity attraction poles initiated by the Belgian-state Federal Services for Scientific Technical and Cultural Affairs.

References

[1] M. El Eid, A.E. Champagne, W. Shaya, in: N. Prantzos, S. Harissopoulos (Eds.), Proc. of Nuclei in the Cosmos V, Frontières, 1999, p. 123.
[2] D.B. Duncan, J.E. Perry, Phys. Rev. 82 (1951) 809.
[3] W.A.S. Lamb, R.E. Hester, Phys. Rev. 108 (1957) 1304.
[4] R.E. Pixley, Ph.D. Thesis, California Institute of Technology, 1957.
[5] D.F. Hebbard, G.M. Bailey, Nucl. Phys. 49 (1963) 666.
[6] U. Schröder et al., Nucl. Phys. A 467 (1987) 240.
[7] P.F. Bertone, A.E. Champagne, D.C. Powell, C. Iliadis, S.E. Hale, V.Y. Hansper, in preparation.
[8] C. Angulo et al., Nucl. Phys. A 656 (1999) 3.
[9] E.G. Adelberger et al., Rev. Mod. Phys. 70 (1998) 1265.
[10] A.M. Lane, R.G. Thomas, Rev. Mod. Phys. 30 (1958) 257.
[11] C. Angulo, P. Descouvemont, Phys. Rev. C 61 (2000) 064611.
[12] F.C. Barker, Nucl. Phys. A 588 (1995) 693.
[13] F. Ajzenberg-Selove, Nucl. Phys. A 523 (1991) 1.
[14] R.J. Holt, H.E. Jackson, R.M. Laszewski, J.E. Monahan, J.R. Specht, Phys. Rev. C 18 (1978) 1962.
[15] D. Baye, E. Brainis, Phys. Rev. C 61 (2000) 025801.
[16] A.M. Mukhamedzhanov, R.E. Tribble, N.K. Timofeyuk, Phys. Rev. C 51 (1995) 3472.
[17] J.C. Fernandes, R. Crespo, F.M. Nunes, Phys. Rev. C 61 (2000) 064616.
[18] F.B. Hagedorn et al., Phys. Rev. 105 (1957) 129.
[19] D.D. Clayton, Principles of Stellar Evolution and Nucleosynthesis, University of Chicago Press, 1983.
[20] G.R. Caughlan, W.A. Fowler, At. Data Nucl. Data Tables 40 (1988) 283.